

Study of the Differential Cross Sections of Deuteron Stripping Reactions as a Function of the Incident Energy*

E. W. HAMBURGER†

University of Pittsburgh, Pittsburgh, Pennsylvania and Universidade de São Paulo, São Paulo, Brasil

(Received March 1, 1961)

Angular distributions for the reactions $C^{12}(d,p)$ and $O^{16}(d,p)$ to the ground and first excited states of C^{13} and O^{17} have been obtained at deuteron energies of 10.2, 12.4, and 14.8 Mev. These results and those of previous experiments at other energies between 3 and 19 Mev are compared with the predictions of the usual plane-wave Born approximation theory, due originally to Butler. The assumption of plane waves leads to the prediction that the differential cross section is a function of energy and scattering angle only through the transfer momentum q : angular distributions at different energies should coincide when plotted vs q . It is found that this is only approximately true on the main stripping peak of the angular distribution; at larger angles the cross section is a more complicated function of energy and angle. Furthermore the stripping peak itself shifts as a function of q , principally in the deuteron energy range 10 to 19 Mev.

I. INTRODUCTION

A. General

THE angular distributions from deuteron stripping reactions on light nuclei at intermediate energies (~ 6 to 20 Mev) show a prominent forward peak whose shape and position can be well accounted for by a direct interaction theory, due originally to Butler.^{1,2} At angles larger than that of the stripping peak the theory usually does not agree with experiment. Although many measurements of stripping angular distributions have been reported, the variation of the cross section with energy has not been studied very often so far—mainly because no variable energy accelerators in the energy range of interest were available. Such measurements should be valuable because their comparison with theoretical predictions can help to elucidate the mechanism of the reactions.

The present article reports on measurements on the $C^{12}(d,p)$ and $O^{16}(d,p)$ reactions to the ground and first excited states of C^{13} and O^{17} , at deuteron energies of 14.8, 12.4, and 10.2 Mev. These results and those of previous experiments at other energies (see Table I) are compared with theory.

The (d,p) reactions on C^{12} and O^{16} are probably the stripping reactions most extensively studied so far. They were chosen for the present work because of general convenience and because the two fastest proton groups in each case can be separated with low resolution. Furthermore the closed shell structure of O^{16} should make the $O^{16}(d,p)O^{17}$ reaction a particularly favorable case for the validity of the simple theory.

B. Theoretical Predictions

The "crude"² stripping theory for the reaction $X(d,p)Y$ to a definite state of Y is based on four main

* Work partially done at the Sarah Mellon Scaife Radiation Laboratory and partially supported by the joint program of the Office of Naval Research and the Atomic Energy Commission.

† Permanent address: Dept. de Física, Faculdade de Filosofia, Universidade de São Paulo, São Paulo, Brasil.

¹ S. T. Butler, Proc. Roy. Soc. (London) **A208**, 559 (1951).

² For a recent review of direct reaction theories, see N. Austern, in *Fast Neutron Physics*, edited by J. B. Marion and J. L. Fowler (Interscience Publishers, Inc., New York, 1961). Sec. V.D.

assumptions:

- (1) The cross section is calculated in Born approximation using plane waves.
- (2) The proton-target interaction is neglected.
- (3) The neutron is captured into a state of definite orbital angular momentum l (shell-model assumption).
- (4) The matrix element integral is taken only over the region of configuration space where the proton is outside a sphere of radius r_0 centered at the target nucleus; r_0 is of the order of magnitude of the nuclear radius.

If we neglect the velocity dependence of the interaction potential and if we assume that r_0 is energy-independent, then it follows from assumption (1) alone that the matrix element is a function of energy and scattering angle through only one parameter, the transfer momentum $q = |\mathbf{K}_d - \mathbf{K}_p|$, where \mathbf{K}_d and \mathbf{K}_p are the incoming deuteron and outgoing proton wave vectors.³ The cross section has an additional weak energy dependence due to the phase-space factor K_p/K_d which multiplies the matrix element.⁴

The other assumptions, (2), (3), and (4), allow one to calculate the precise form of the dependence of the cross section on q . One finds a function which has a large peak at some small value of q , $q \sim 0.3$ ⁵ and smaller peaks at larger values of q . Now q is a monotonically increasing function of the scattering angle θ :

$$q^2 = K_p^2 + K_d^2 - 2K_p K_d \cos\theta,$$

and the peak at small q corresponds to a peak in the angular distribution at small θ . When the deuteron energy is decreased, the θ corresponding to a given q (and therefore to a given cross section) increases; consequently the angular distribution predicted by the theory shifts towards larger angles when the energy is

³ The expression given for q assumes the target mass to be infinite; the correct expression, used in the computations in the present work, is $q = |\mathbf{K}_d - [A/(A+1)]\mathbf{K}_p|$, where A is the mass number of the target.

⁴ K_p/K_d increases by 10% from $E_d = 19$ to 8 Mev, and by 25% from 19 to 4 Mev, for the C^{13} g.s. group, and changes much less for the other three groups.

⁵ The unit of length is 10^{-13} cm = 1 fermi.

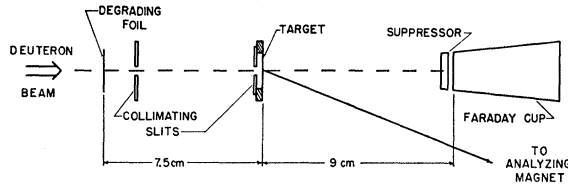


FIG. 1. Schematic diagram of the beam energy degrading system, target and Faraday cup.

decreased, without changing its shape appreciably. For example, the $C^{12}(d,p)C^{13}$ ground-state (g.s.) angular distribution should shift by $\sim 2.5^\circ$ when the deuteron energy E_d changes from 14.8 to 12.4 Mev. However if the differential cross section is plotted vs q (q plot) instead of vs θ , the cross sections measured at different energies should coincide. We emphasize again that this

TABLE I. Angular distribution measurements on the $C^{12}(d,p)C^{13}$ and $O^{16}(d,p)O^{17}$ reactions at deuteron energies above ~ 3 Mev.

Deuteron lab energy (Mev)	Quoted error in absolute σ	Authors	Reference
$C^{12}(d,p)C^{13}$			
1.8 to 3.3	5–10%	McEllistrem <i>et al.</i>	a
3.29	10%	Holmgren <i>et al.</i>	b
2.84 to 4.75	not quoted	Bonner <i>et al.</i>	c
4.65, 7.15	30%	Zaika <i>et al.</i>	d
8	not quoted	Rotblat	e
9	10%	Green and Middleton	f
9.55	30%	Zaika <i>et al.</i>	d
10.2, 12.4	25%	Present work	
12.1, 13.3	30%	Zaika <i>et al.</i>	d
14.8	20%	McGruer <i>et al.</i> , Mayo and Hamburger, and present work	g
14.9, 16.6, 18.1, 19.6	20%	Morita <i>et al.</i>	h
19	$\sim 5\%$	Freemantle <i>et al.</i>	i
$O^{16}(d,p)O^{17}$			
2.1	10%	Grosskreutz	j
3.43	10%	Stratton <i>et al.</i>	k
3.49 to 4.11	$\sim 15\%$	Baumgartner and Fulbright	l
7.73	$\sim 6\%$	Burge <i>et al.</i> and Holt and Marsham	m, n
9	absolute σ not measured	Green and Middleton	f
10.2	30%	Present work	
12.4	25%	Present work	
14.8	25%	Keller and present work	o
19	8%	Freemantle <i>et al.</i>	p

^a M. T. McEllistrem *et al.*, Phys. Rev. **104**, 1008 (1956).

^b H. D. Holmgren *et al.*, Phys. Rev. **95**, 1544 (1954).

^c T. W. Bonner *et al.*, Phys. Rev. **101**, 209 (1956).

^d N. I. Zaika *et al.*, J. Exptl. Theoret. Phys. (U.S.S.R.) **39**, 3 (1960) [translation: Soviet Phys.—JETP **12**, 1 (1961)].

^e J. Rotblat, Nature **167**, 1027 (1951).

^f T. S. Green and R. Middleton, Proc. Phys. Soc. (London) **A69**, 28 (1956).

^g J. N. McGruer *et al.*, Phys. Rev. **100**, 235 (1955). See also reference 8.

^h S. Morita *et al.*, J. Phys. Soc. Japan **15**, 550 (1960).

ⁱ R. G. Freemantle *et al.*, Phil. Mag. **45**, 1200 (1954).

^j J. C. Grosskreutz, Phys. Rev. **101**, 706 (1956).

^k T. F. Stratton *et al.*, Phys. Rev. **98**, 629 (1955).

^l E. Baumgartner and H. W. Fulbright, Phys. Rev. **107**, 219 (1957).

^m E. J. Burge *et al.*, Proc. Roy. Soc. (London) **A210**, 534 (1951).

ⁿ J. R. Holt and T. N. Marsham, Proc. Phys. Soc. (London) **A66**, 1032 (1953).

^o E. L. Keller, Phys. Rev. **121**, 820 (1961). The data shown in the figures are from the preliminary results of this work. The final results are slightly different, but for the purposes of this paper the difference is unimportant.

^p R. G. Freemantle *et al.*, Phys. Rev. **92**, 1268 (1953).

prediction of the theory is a consequence only of the plane wave assumption (1) and of the assumption of constant r_0 .

The principal aim of the present work was to test this particular prediction of the theory and thereby test assumption (1).

II. EXPERIMENTAL PROCEDURE

The external deuteron beam from the University of Pittsburgh cyclotron is focused and analyzed by two magnetic spectrometers before hitting the target. The reaction products are selected by a third magnetic spectrometer which can be rotated about the target, and are detected in nuclear emulsions.^{6,7} The emulsions were covered with aluminum foil so that deuterons and other particles were stopped and only protons produced tracks.

The energy of the beam from the cyclotron varies in the range 14.7–14.9 Mev, according to the tuning. Previous experience indicated that the stripping cross sections do not vary appreciably in this interval. In order to vary the energy by larger amounts, tantalum absorber foils were inserted in the beam path. These foils cause two important side effects: (1) the energy spread of the beam is increased: the over-all resolution changed from ~ 70 kev at full beam energy to ~ 200 kev at 12.4 Mev and ~ 300 kev at 10.2 Mev. (2) Multiple scattering makes the beam fan out. In order to

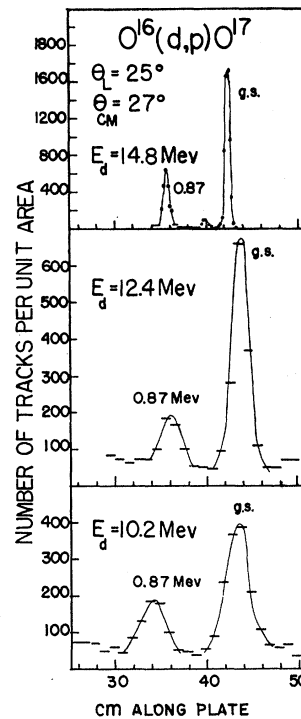


FIG. 2. Typical raw data for the $O^{16}(d,p)O^{17}$ reaction at $\theta_L = 25^\circ$. The number of tracks per (arbitrary) unit area is plotted vs distance along the plate, in centimeters.

⁶ R. S. Bender *et al.*, Rev. Sci. Instr. **23**, 542 (1952).

⁷ E. W. Hamburger, Ph.D. thesis, University of Pittsburgh, 1959 (unpublished).

have reasonable beam intensity the target must then be close behind the degrading foil. On the other hand, a collimator must be inserted between the foil and the target, in order to define the incident beam direction and to make possible the collection of the beam in a Faraday cup behind the target.

Figure 1 shows the experimental arrangement. The foils could be changed without breaking the vacuum. The collimating slits were 1.6 mm wide, 12 mm high and ~ 50 mm apart, allowing maximum scattering angles of $\sim 2^\circ$ horizontally and $\sim 14^\circ$ vertically. The Faraday cup collected all particles scattered by less than 3° horizontally and 8° vertically. A few percent of the incoming particles were therefore not collected in the Faraday cup. The reproducibility of the data, and in particular the reliability of the cup as a monitor, were checked by making exposures with the degrading foils at different distances from the collimator. The results were consistent within $\pm 10\%$ in the carbon work and in the oxygen work at 12.4 Mev, but a difference of 20% appeared in one of the oxygen exposures at 10.2 Mev.

The collimator reduced the cross-sectional area of the beam by a factor 4 and insertion of the thicker foil reduced the intensity by another factor 5. However the cross sections are large and the total cyclotron running time was only a few days.

The targets were ~ 2 mg/cm² thick. The carbon target was polyethylene sheet coated on both sides with ~ 0.05 mg/cm² silver. The oxygen targets were NiO, prepared by J. C. Armstrong by completely oxidizing a Ni foil. The background produced by the nickel in the oxygen exposures was appreciable only at large

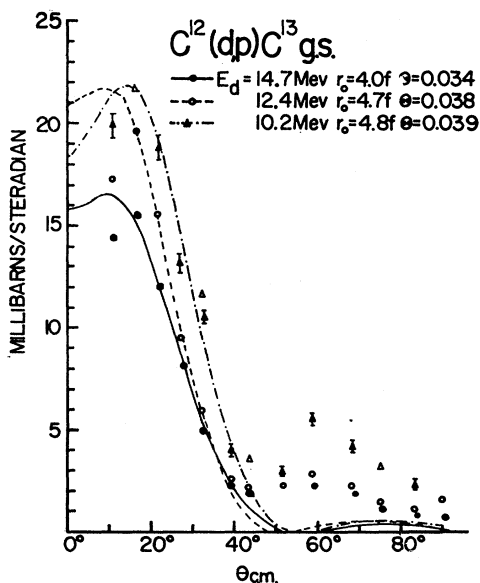


FIG. 3. Angular distributions for the $C^{12}(d,p)C^{13}$ g.s. reaction at $E_d=14.7$, 12.4, and 10.2 Mev, with theoretical stripping curves.

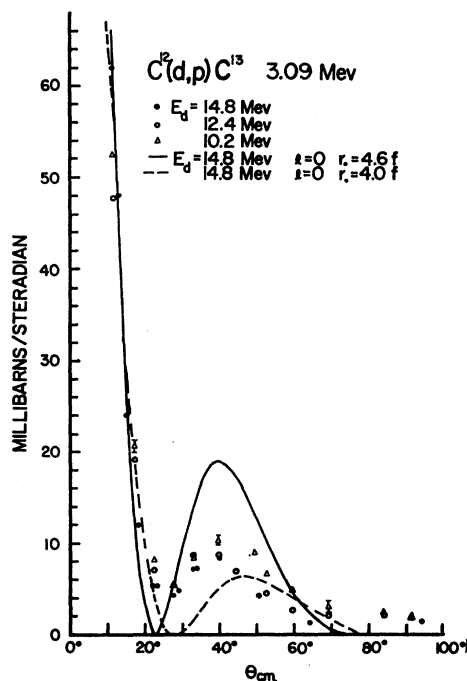


FIG. 4. Angular distributions for the $C^{12}(d,p)C^{13}$ 3.09-Mev reaction at $E_d=14.8$, 12.4 and 10.2 Mev. The two theoretical curves at 14.8 Mev show that the data at small angles can be fit by a wide range of theoretical curves.

angles. No background was observed in the carbon work, showing that proton production in the degrading foil was negligible, as expected for a heavy element such as tantalum. Typical spectra are shown in Fig. 2.

The absolute cross section of the $C^{12}(d,p)C^{13}$ g.s. reaction at $E_d=14.8$ Mev has been measured previously to be 15.5 mb/sr $\pm 20\%$ at the peak of the angular distribution.⁸ The $O^{16}(d,p)O^{17}$ g.s. peak cross section, measured relative to the above, is 34 mb/sr $\pm 25\%$.⁷ These two cross sections were taken as references in the present work, in which only relative cross sections were measured. The error in the relative cross sections is estimated to be less than $\pm 10\%$ for the carbon groups; for the oxygen groups it is estimated to be less than $\pm 15\%$ at $E_d=14.8$ and 12.4, and less than $\pm 20\%$ at 10.2 Mev.

III. RESULTS AND DISCUSSION

A. Stripping Reduced Width and Radius as a Function of Energy

Figures 3 to 6 show the data obtained at 14.8 Mev (data from references g and o in Table I and from the present work), 12.4 and 10.2 Mev. Theoretical stripping curves have been compared with the data and reduced widths Θ^2 have been extracted.⁹ These parameters are

⁸ S. Mayo and E. W. Hamburger, Appendix A of reference 7.

⁹ The method of extracting reduced widths is discussed by M. H. Macfarlane and J. B. French, Revs. Modern Phys. 32, 567 (1960).

TABLE II. Parameters of stripping curves.

	l	$E_d=10.2$ Mev		$E_d=12.4$ Mev		$E_d=14.8$ Mev	
		r_0	Θ^2	r_0	Θ^2	r_0	Θ^2
$O^{16}(d,p)O^{17}$, g.s.	2	6.2 ± 0.2	0.034 ± 0.003	5.6 ± 0.3	0.047 ± 0.004	5.5 ± 0.2	0.055 ± 0.005
$O^{16}(d,p)O^{17}$, 0.87 Mev	0	5.3 ± 0.3	0.13 ± 0.02	5.3 ± 0.3	0.14 ± 0.02	4.9 ± 0.3	0.16 ± 0.05
$C^{12}(d,p)C^{13}$, g.s.	1	4.7 ± 0.3	0.039 ± 0.003	4.6 ± 0.3	0.038 ± 0.003	4.0 ± 0.2	0.034 ± 0.003

given in Table II with the uncertainties due only to the ambiguities of the fits. No parameters were extracted for the $C^{12}(d,p)C^{13}$ 3.09-Mev group: there are too few experimental points at small angles.

The table shows that, for all groups r_0 increases as the energy is decreased. This is because the angular distributions do not shift toward larger angles as the energy is decreased (see following sections): instead of shifting, the stripping peak just grows as the energy decreases, in this energy region. The increase in r_0 is 10 to 20% when E_d changes from 15 to 10 Mev.

The reduced widths depend on the absolute cross sections and are therefore more sensitive to experimental errors. Within the quoted precision of the measurements the reduced widths of the O^{17} 0.87-Mev and C^{13} ground-state groups are constant, although Θ^2 for the latter group seems to increase slightly with decreasing energy ($\sim 10\%$ from 15 to 10 Mev). The value 0.039 for this group at 10.2 Mev agrees well with the value 0.042 extracted⁹ from the 9 Mev data (Table I, reference f).

The O^{17} ground-state reduced width decreases with

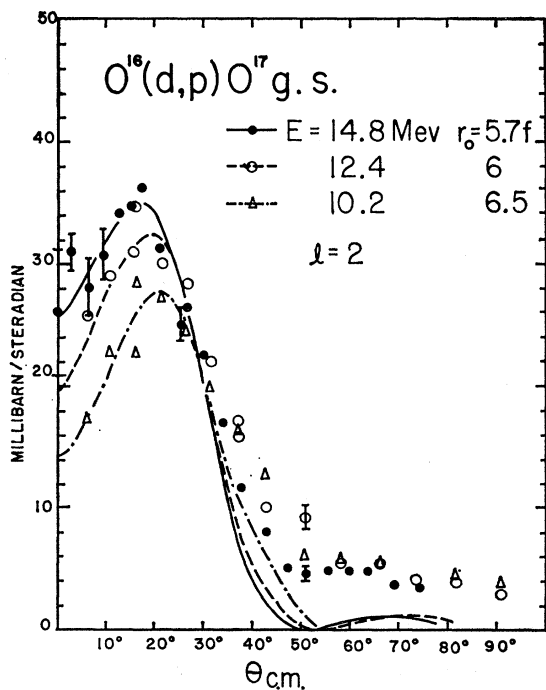


FIG. 5. Angular distributions for the $O^{16}(d,p)O^{17}$ g.s. reaction at $E_d=14.8$, 12.4, and 10.2 Mev, with theoretical stripping curves.

increasing energy, by $\sim 40\%$ from 10 to 15 Mev. However, the reduced width extracted⁹ from the 7.7-Mev data (Table I, m,n) is as large as that at 14.8 Mev, so that it seems that Θ^2 goes through a minimum at ~ 10 Mev. More accurate data are needed, however, before this conclusion can be definitely drawn.

B. Positions of the Maxima and Minima in the Angular Distributions at Different Energies

In this section we examine the energy variation of qualitative features of the angular distributions, viz., the positions of the peaks and valleys. Such a discussion has the advantage that it depends only on the shapes of the angular distributions and not on the comparison

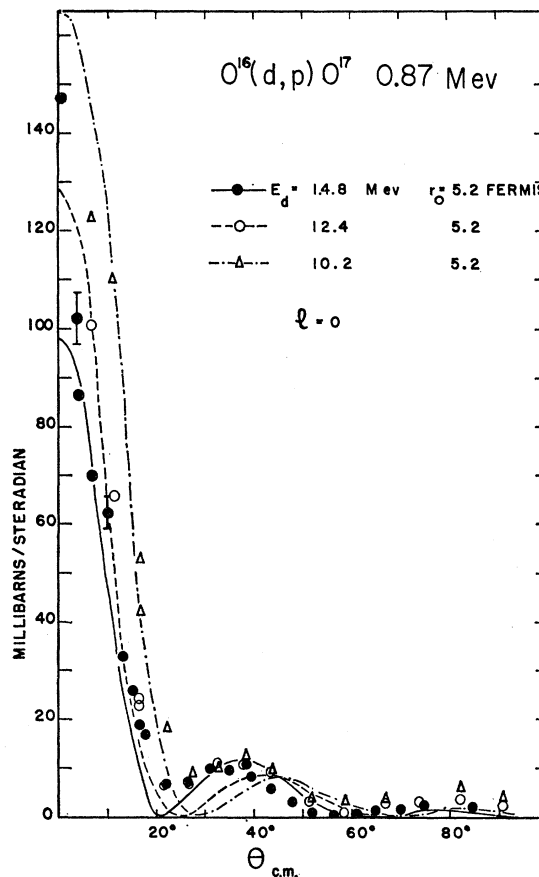


FIG. 6. Angular distribution for the $O^{16}(d,p)O^{17}$ 0.87-Mev reaction, at $E_d=14.8$, 12.4, and 10.2 Mev, with theoretical stripping curves.

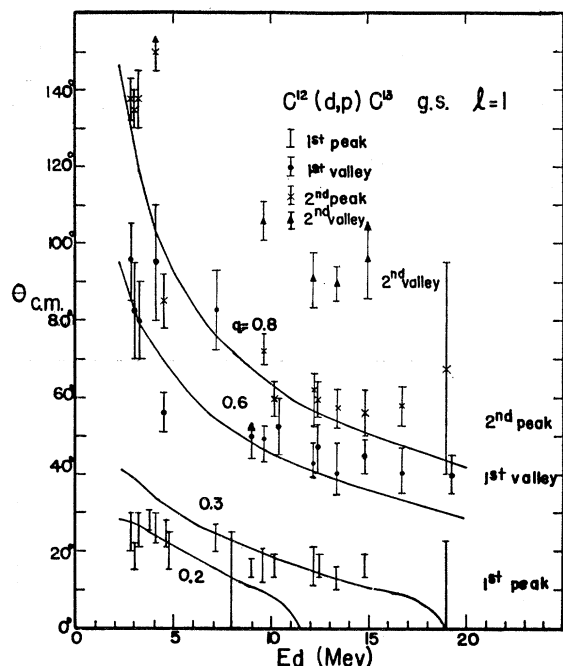


FIG. 7. $C^{12}(d,p)C^{13}$ g.s. Position of the peaks and valleys in the angular distributions as a function of deuteron energy.

of cross sections measured at different energies (and at different laboratories), which are experimentally less certain. Furthermore the discussion can include data down to very low deuteron energies, where sharp resonances occur, because the resonances usually do not shift the positions of the peaks by more than 10° .

Figures 7 to 10 show the positions of the maxima and minima as a function of deuteron energy for the four groups studied. References are given in Table I and some of the data are reproduced in Figs. 11-14; estimated uncertainties are given. Also shown are curves giving the angle of constant transfer momentum q as a function of energy. If the "crude" theory outlined in the Introduction were correct, all points corresponding to a given maximum (or minimum) should fall on one such curve. The figures show that for deuteron energies between 3 and 9 Mev the points follow such a curve approximately. For energies above 10 Mev, however, *all* the peaks and valleys shift much less than predicted by the curves. Consequently curves which fit the points at low energies fall below the high-energy points. The O^{17} ground-state group is an exception, in which the lack of shifting above 10 Mev appears to be compensated by a large shift between 9 and 10 Mev.

C. Detailed Comparison with the Plane Wave Assumption

In order to verify whether q is the only important parameter, we plot in Figs. 15-18 the measured differential cross sections from this and previous experiments vs q . Figures 11-14 show the same data plotted vs

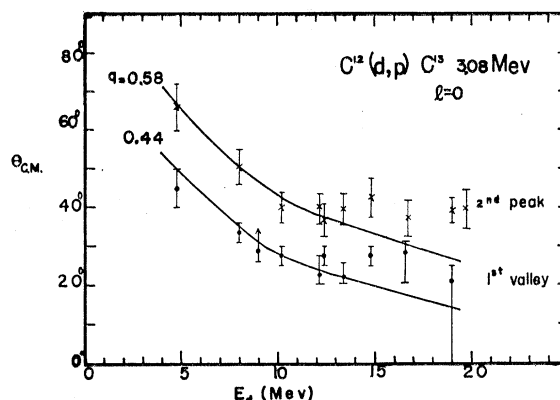


FIG. 8. $C^{12}(d,p)C^{13}$ 3.09 Mev. Position of the peaks and valleys in the angular distributions as a function of deuteron energy.

center-of-mass (c.m.) scattering angle $\theta_{c.m.}$. References are given in Table I. Not all the available data are shown; in particular, the recent experiments of Morita *et al.* (Table I), and of Zaika *et al.* (Table I) on $C^{12}(d,p)C^{13}$ were not included.

A first glance at the graphs reveals two significant points: (i) the order of magnitude of the cross sections is the same at all energies, indicating the predominance of direct interactions over resonance processes. (ii) Although the data plotted vs q do not fall on a single line, as predicted by plane wave theory, they do tend to "bunch" closer together than on the $\theta_{c.m.}$ graph. This was to be expected, since plane wave theory yields approximately correct results for the angular distributions.

We now discuss each group:

(a) The C^{13} ground-state group ($l=1$), Fig. 15, shows good agreement with plane wave theory on the slope of the stripping peak, $0.3 < q < 0.5$, for all energies. There are three sets of data which disagree with the "universal" curve obtained for this reaction at the stripping peak: (α) The data of Bonner *et al.* (Table I) at 4.51 Mev; no error is quoted on the cross sections in this experiment. The data may be compared to that of Holmgren *et al.* (Table I) which give a cross section 1.6 times larger than that of Bonner *et al.* at 3.29 Mev and 30° . If we accept the Holmgren *et al.* (Table I) measurement as being correct (the quoted error is 10%) and

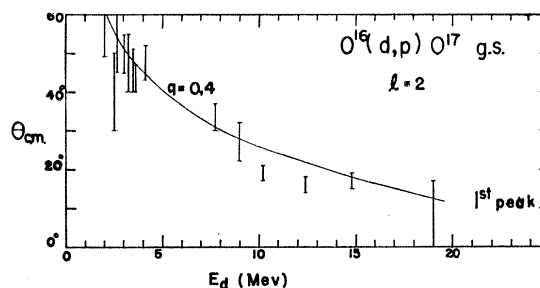


FIG. 9. $O^{16}(d,p)O^{17}$ g.s. Position of the peaks and valleys in the angular distributions as a function of deuteron energy.

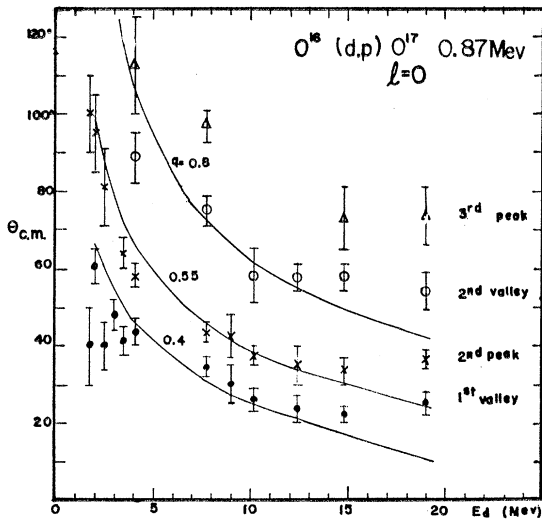


FIG. 10. $O^{16}(d,p)O^{17}$ 0.87 Mev. Position of the peaks and valleys in the angular distributions as a function of deuteron energy.

multiply the data of Bonner *et al.* by a factor 1.6, very good agreement is obtained, as shown in Fig. 15. (β) The data of Rotblat at 8 Mev; again no errors are quoted on the absolute cross section. If we multiply the cross section by a factor 0.75 very good agreement is obtained, as shown in Fig. 15. (γ) The data of Zaika *et al.* (Table I); the quoted error on the absolute cross section is $\pm 30\%$. The cross sections at the peaks of the angular

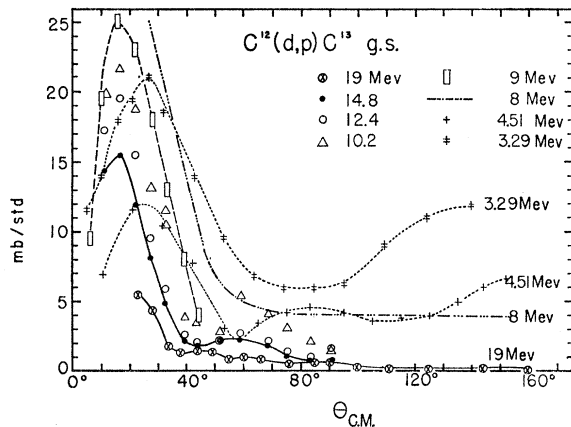


FIG. 11. $C^{12}(d,p)C^{13}$ g.s. Measured differential cross sections at several deuteron energies vs center-of-mass scattering angle. References in Table I.

distributions are given as 13, 14, and 18 mb/sr for $E_d=13.3$, 12.1 and 9.55 Mev, respectively, about 30% lower than the values which would be expected at these energies by interpolation from the results of the present work. Such a difference is well within the quoted errors of the experiments. At the lowest energy, 7.15 Mev, Zaika *et al.* (Table I) give a peak cross section which agrees with the data of Fig. 11 without the need

of a normalization factor. In order to obtain agreement, therefore, we must suppose that the cross sections measured by Zaika *et al.* at their lowest energy are in error relative to their high-energy measurements by 30%.

In Sec. B we showed that the position of the stripping peak does not shift along a constant q curve (see Fig. 7). Therefore, the peak position must shift on a σ vs q plot, as shown in Fig. 15. It is interesting to note, however, that this shift of the maximum in Fig. 15 does

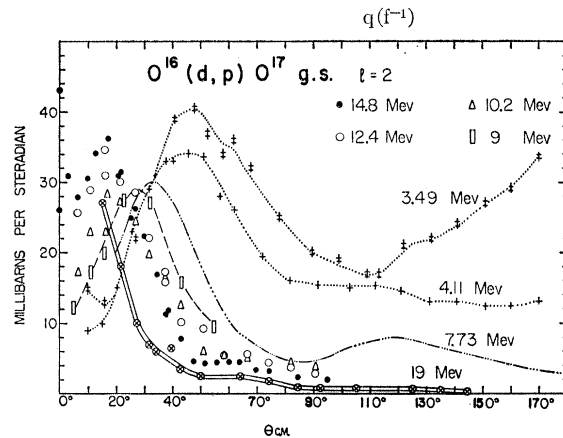


FIG. 12. $O^{16}(d,p)O^{17}$ g.s. Measured differential cross sections at several deuteron energies plotted vs center-of-mass scattering angle. References in Table I.

not correspond to a shift of the peak as a whole; the slope, as we have just seen, remains fixed. It is only the point at which the data break away from the constant slope region that shifts, as illustrated in Fig. 19. The same behavior is responsible for the change in the value of the peak cross section, which in turn causes the change in reduced width with energy.

At large q values, $q > 0.55$, the agreement is much poorer. In general the cross section at a given q in this region tends to increase with decreasing energy. The secondary peak at $q \sim 0.8$ shifts to lower q and increases

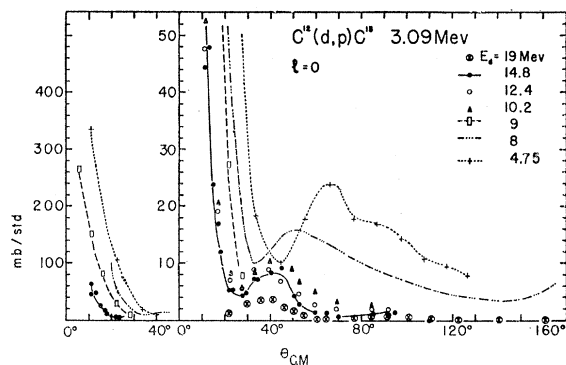


FIG. 13. $C^{12}(d,p)C^{13}$ 3.09 Mev. Measured differential cross sections at several deuteron energies plotted vs center-of-mass scattering angle. References in Table I.

between 19 and 10 Mev but disappears at 8 Mev. At low energies the cross section shows a large backward rise which does not exist at 8 Mev or above 15 Mev. It does not seem to be related to the diffraction-like peak which appears at $\sim 120^\circ$ at 14.9, 13.3, 12.1 and 9.55 Mev. This diffraction peak appears rather suddenly between 8 and 9.55 Mev, as remarked by Zaika *et al.* (Table I). At higher energies it gradually diminishes until it has essentially disappeared at 16.6 Mev.

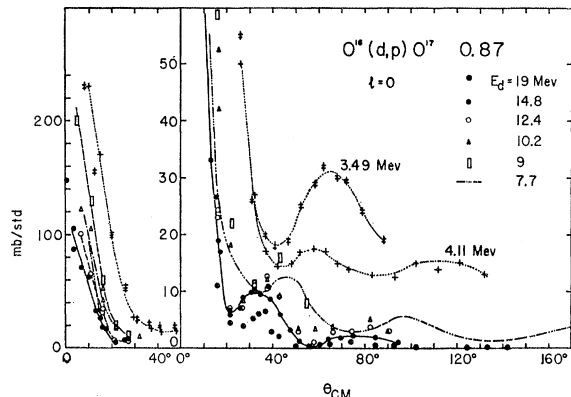


FIG. 14. $O^{16}(d,p)O^{17}$ 0.87 Mev. Measured differential cross sections at several deuteron energies plotted vs center-of-mass scattering angle. References in Table I.

(b) The O^{17} ground-state group ($l=2$), Figs. 12 and 16, shows good agreement with plane wave theory on the whole stripping peak ($0.1 < q < 0.6$), for all energies (at 9 Mev no absolute cross section was measured; the data were normalized to agree with the neighboring energies). For energies above 8 Mev the agreement extends to $q \sim 1.0$, although the 19-Mev data are systematically lower than the 8, 10.2, 12.4, and 14.8-Mev data, which approximately agree. The 8-Mev data show a secondary peak at $q \sim 1.2$ which the other data do not show. The position of the main stripping peak shifts somewhat on the q plot because the peak in the θ plot does not shift enough (see Sec. B); in particular,

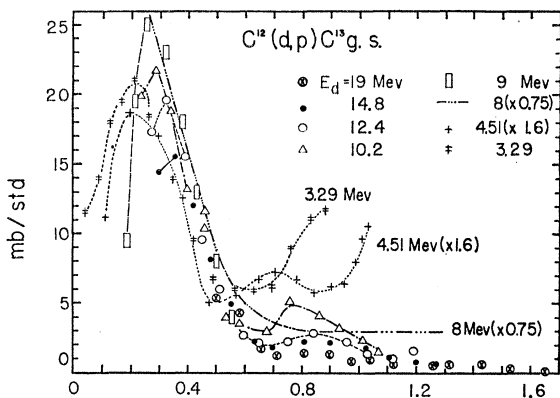


FIG. 15. $C^{12}(d,p)C^{13}$ g.s. Data of Fig. 11 plotted vs transfer momentum q . The measurements at 4.51 and 8 Mev have been multiplied by factors of 1.6 and 0.75, respectively (see text).

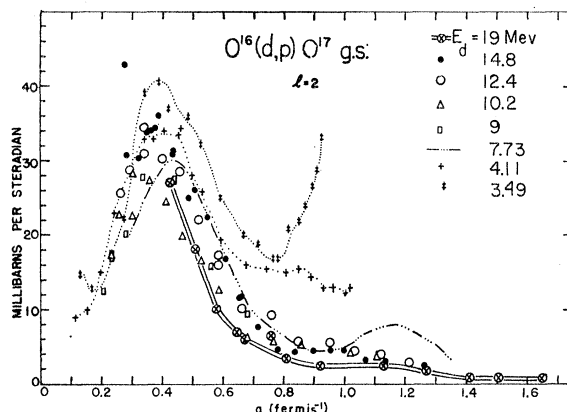


FIG. 16. $O^{16}(d,p)O^{17}$ g.s. Data of Fig. 12 plotted vs transfer momentum q .

we see the sudden shift toward smaller q from 9 to 10 Mev, and the gradual shifting back toward higher q between 10 and 15 Mev. The slope of the peak also shifts: the behavior is different from that of the C^{13} ground-state group discussed in the preceding paragraph.

(c) The two $l=0$ groups corresponding to the first excited states of C^{13} and O^{17} , Figs. 13, 14, 17, and 18, show similar behavior. The slope of the main stripping peak moves towards larger angles on the θ plot as the energy is decreased; however, it does not move as fast as predicted by the theory, so that on the q plot it moves towards smaller q as the energy is decreased.

The secondary peaks grow as the energy is decreased, principally at low energies. They also shift toward lower q values from 19 to 10 Mev, but remain at about the same q (~ 0.5) below 10 Mev. The O^{17} 0.87-Mev group shows a third peak at $q \sim 1.0$, which also grows and shifts towards smaller q as the energy is decreased. Above 13 Mev the C^{13} group also has a third peak, at $\sim 100^\circ$ (references d, h, Table I). This peak (not shown in Fig. 8) does shift to smaller angles as the energy is increased, approximately as predicted by the plane-

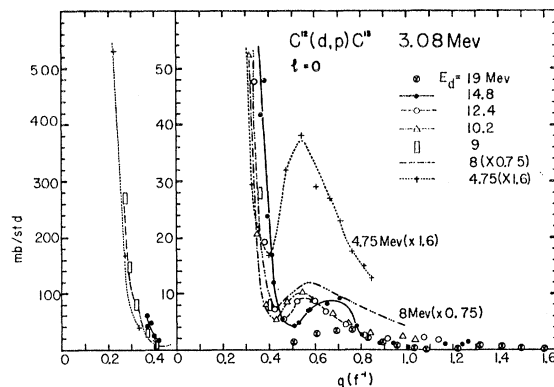


FIG. 17. $C^{12}(d,p)C^{13}$ 3.09 Mev. Data of Fig. 13 plotted vs transfer momentum q . The measurements at 4.75 and 8 Mev have been multiplied by factors of 1.6 and 0.75, respectively (see text).

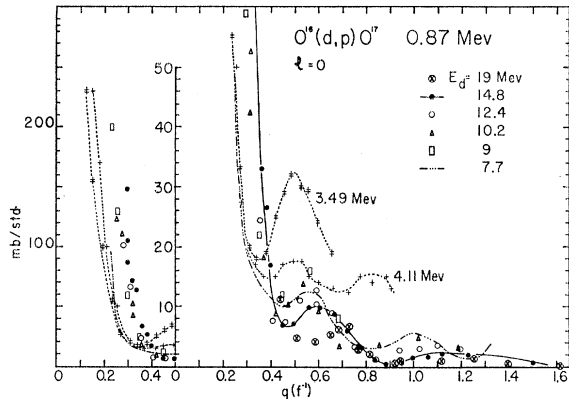


FIG. 18. $O^{16}(d,p)O^{17}$ 0.87 Mev. Data of Fig. 14 plotted vs transfer momentum q .

wave theory. It is interesting that for the $l=0$ transitions the structure in the angular distribution at large angles does not disappear when the energy is increased, as it does for the C^{13} ground-state group ($l=1$). The shifting of the peaks in the q plot is of course related to the lack of shifting in the θ plot, discussed in Sec. B. It can be approximately compensated for, in the crude theory, by an increase of the cutoff radius r_0 with decreasing energy. The change in the height of the peaks, however, cannot be explained by this theory.

D. Conclusion

The transfer momentum q is the dominating parameter on the stripping peak. At larger angles the cross section has a more complicated angular and energy dependence, principally at low energies. Two of the results seem specially significant: the lack of shifting of the angular distributions on the θ plots at energies above 10 Mev, and the growth of the cross section at large angles when the energy is decreased. The plane

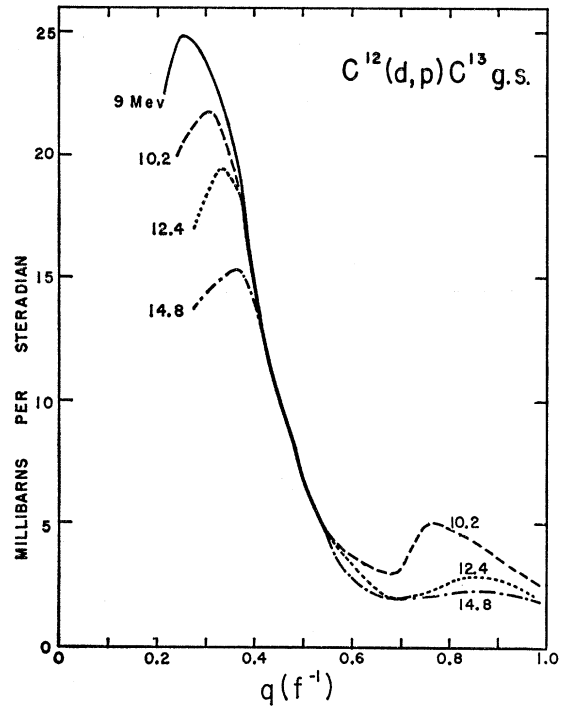


FIG. 19. Illustration of the behavior of the $C^{12}(d,p)C^{13}$ g.s. differential cross section.

wave assumption (1) appears to represent only a first crude approximation to the true wave functions.

ACKNOWLEDGMENTS

The author gratefully acknowledges the extensive help of A. I. Hamburger in the analysis of the data and the help of A. G. Blair and S. Micheletti in the data collection. He thanks E. L. Keller for permission to use unpublished results and J. C. Armstrong for loan of the oxygen targets.